Endothelin-1 potentiates TRPV1-mediated vasoconstriction of human adipose arterioles in a protein kinase C-dependent manner

Ankush M Korishettar[1,2], Yoshinori Nishijima[2,3], Zhihao Wang[3,6], Yangjing Xie[3,7], Juan Fang[4,5], David A. Wilcox[4,5], David X. Zhang[1,2,3]

[1]Department of Pharmacology and Toxicology, [2]Cardiovascular Center and [3]Department of Medicine, [4]Department of Pediatrics, Medical College of Wisconsin and [5]Children's Research Institute, The Children's Hospital of Wisconsin, Milwaukee, WI, USA.
[6]Department of Geriatrics, The First Hospital of Jilin University, Changchun, 130021, China
[7]Department of Cardiology, The First Affiliated Hospital of Anhui Medical University, Hefei, 230032, China

Running title: ET-1 potentiates TRPV1-mediated vasoconstriction of human arterioles

Word count: 3592

Data availability statement: Data available on request from the authors. The data that support the findings of this study are available from the corresponding author upon reasonable request. Some data may not be made available because of privacy or ethical restrictions.

Address correspondence to:
Ankush M. Korishettar
Department of Pharmacology and Toxicology
Cardiovascular Center
Medical College of Wisconsin
8701 Watertown Plank Rd
Milwaukee, WI 53226
Phone: (414) 446-1527
E-mail: akorishettar@mcw.edu

Abstract

Background and Purpose: Vascular transient receptor potential vanilloid (TRPV) channels have emerged as important regulators of vascular tone. TRPV1 and endothelin-1 (ET-1) are independently associated with the pathophysiology of coronary vasospasm but the relationship between their vasomotor functions remains unclear. We characterized the vasomotor function of TRPV1 channels in human arterioles and investigated regulation of their vasomotor function by ET-1.

Experimental Approach: Arterioles were threaded on two metal wires, equilibrated in a physiological buffer at 37 ^{o}C and exposed to increasing concentrations of capsaicin in the absence or presence of SB366791 (TRPV1-selective inhibitor) or GF109203X (protein kinase C (PKC)-selective inhibitor). Some arterioles were preconstricted with ET-1 or phenylephrine or high potassium buffer. TRPV1 mRNA and protein expression in human arteries were also assessed.

Key Results: TRPV1 transcripts and proteins were detected in human resistance arteries. Capsaicin (1 μM) induced concentration-dependent constriction of endothelium-intact (35 ± 8 %) and endothelium-denuded (43 ± 11 %) human adipose arterioles (HAA), which was significantly inhibited by SB366791 (0.2 ± 0.1 %). Preconstriction of HAA with ET-1, but not high potassium buffer or phenylephrine, significantly potentiated capsaicin-induced constriction (33 ± 7 % vs 12 ± 8 %). GF109203X significantly inhibited potentiation of capsaicin-induced constriction by ET-1.

Conclusion and Implications: TRPV1 channels are expressed in the human vasculature and can influence vascular tone of human arterioles upon activation. Their vasomotor function is modulated by ET-1, mediated in part by PKC. These findings reveal a novel interplay between ET-1 signaling and TRPV1 channels in human VSMC, adding to our understanding of the ion channel mechanisms that regulate human arteriolar tone and may also contribute to the pathophysiology of coronary vasospasm.

Keywords: transient receptor potential vanilloid; endothelin-1; human arterioles; vasoconstriction; potentiation

Abbreviations

CAD (coronary artery disease)

EC (endothelial cells)

HAA (human adipose arterioles)

HCA (human coronary arterioles)

High-K^+ PSS (high potassium physiological saline solution)

mGFP (monomeric green fluorescent protein)

MLC (myosin light chain)

NFDM (non-fat dry milk)

VSMC (vascular smooth muscle cells)

Introduction

The transient receptor potential family of ion channels have emerged as physiological Ca^{2+} entry pathways in vascular cells and as important regulators of vascular tone. These non-selective, Ca^{2+}-permeable cation channels mediate physiological processes such as membrane potential regulation (Gonzales et al., 2010; Gonzales and Earley, 2013), ligand-operated (Sullivan and Earley, 2013) and receptor-operated (Peppiatt-Wildman et al., 2007; Liu et al., 2009) Ca^{2+} entry, myogenic vasoconstriction (Spassova et al., 2006; Gonzales et al., 2014) and flow-induced vasodilation (Hartmannsgruber et al., 2007; Bubolz et al., 2012). They also contribute to vascular pathologies such as hypertension, vascular remodeling, pulmonary edema and ischemia/reperfusion injury (Inoue et al., 2006; Earley and Brayden, 2015).

TRPV1, the first identified member of the TRPV subfamily, plays a role in thermosensation, nociception, osmoreception and mechanosensation (Baylie and Brayden, 2011). Although historically, neuronal TRPV1 has a well-established role in pain and neurogenic inflammation, the expression and function of TRPV1 in non-neuronal tissues is becoming increasingly apparent (Fernandes et al., 2012). Within the vasculature, TRPV1 is expressed in endothelial cells (EC) (Bratz et al., 2008; Yang et al., 2010), vascular smooth muscle cells (VSMC) (Kark et al., 2008) and innervating perivascular sensory nerves (Tóth et al., 2005). TRPV1 activation on each cell-type produces different vasomotor responses. While endothelial/neuronal TRPV1 activation elicits vasodilation of arterioles (Wang et al., 2006; Bratz et al., 2008; Yang et al., 2010), vascular smooth muscle TRPV1 activation induces vasoconstriction (Pórszász et al., 2002; Kark et al., 2008; Czikora et al., 2012). Similarly, vascular bed- and species-specific differences also exist in the vasomotor responses evoked by TRPV1 activation (Kark et al., 2008; Earley and Brayden, 2015). Although extensively characterized in animal models, the vasomotor function of TRPV1 in the human vasculature remains understudied.

Recent clinical case studies report the occurrence of coronary vasospasm (Akçay et al., 2009; Sogut et al., 2012) and thunderclap headache (Boddhula et al., 2018) in human subjects, after prolonged exposure to a capsaicin-patch or due to overconsumption of capsaicin - contained in hot chili peppers. These incidents implicate TRPV1 channels in the pathogenesis of vasospasm. It remains unclear whether capsaicin-induced vasospasm in humans is due to a direct effect on the

vasculature or due to an indirect effect on sympathetic tone. Moreover, the factors that may modulate capsaicin vasomotor effects remain elusive. In the present study, we have characterized the functional expression of TRPV1 channels in human adipose and coronary resistance arteries and arterioles and determined the mechanism of TRPV1-mediated vasomotor effects. We have also studied the interaction between ET-1 and TRPV1 vasomotor functions and its effects on human arteriolar contractility.

Methods

Human tissue acquisition

As described previously (Nishijima et al., 2016), fresh human adipose and atrial tissues (n=50 and n=7 respectively) were obtained as discarded surgical specimens from a total of 57 patients undergoing abdominal surgeries or cardiopulmonary by-pass procedures and unused whole hearts (n=6) were obtained from Donor Network. After surgical removal, specimens were placed in ice-cold HEPES buffer (in mM; 138 NaCl, 4 KCl, 1.6 $CaCl_2$, 2 $MgSO_4$, 1.2 KH_2PO_4, 6 glucose and 10 HEPES) (pH 7.4) or in a cardioplegic buffer solution (for heart tissue) and transferred to the laboratory for isolated vessel studies. De-identified patient demographic data were collected using the Generic Clinical Research Database at the Medical College of Wisconsin. All protocols were approved by the Institutional Review Board of the Medical College of Wisconsin and Froedtert Hospital.

Patients with no or up to one risk factor for coronary artery disease (CAD) (eg. hypertension/hyperlipidemia) were primarily included in this study and together constituted the non-CAD group. Due to the low availability of non-CAD coronary tissues, human coronary arteries from patients clinically diagnosed with CAD were utilized in selected studies. Human coronary tissues were primarily utilized to complement and extend findings from the human adipose vascular bed to the human coronary vascular bed. Subjects were not pre-selected and all data were included for statistical analysis once control response(s) on each vessel passed predefined criteria. Patient demographics data are summarized in Table 1.

Cell culture and transfection

HEK-293 cells, between passages 6 and 10, were provided by Dr. David Wilcox (Medical College of Wisconsin) and grown in Dulbecco's Modified Eagle Medium (DMEM) supplemented with 10 % FBS, 100 U/mL penicillin G and 100 µg/mL streptomycin at 37 °C and 5 % CO_2.

The full-length human TRPV1 (hTRPV1; NM_080704.3) cDNA clone was obtained from Origene (Rockville, MD) and subcloned into pCMV6 mammalian expression vectors, resulting in a TRPV1 fusion protein with its COOH-terminus tagged with a monomeric green fluorescent protein (mGFP). The hTRPV1-mGFP construct was then excised from pCMV6 and subcloned into an HIV type-1 vector, pWPTS-GFP (gift from D. Trono, University of Geneva, Switzerland), replacing the GFP cDNA cassette. The nucleic acid sequence of hTRPV1-mGFP constructs was

verified by direct DNA sequencing. hTRPV1-mGFP coding plasmids were isolated by an endotoxin-free plasmid kit (Qiagen) and transiently transfected into HEK cells using the lipid-mediated lipofectamine 2000 kit (Invitrogen) according to the manufacturer's protocols. In brief, cells were plated in 60-mm petri dishes 16-24 h before transfection. Cells were transfected with 2 μg plasmid DNA/60-mm dish and used 24-48 h after transfection (Nishijima et al., 2016).

Enzymatic isolation of vascular cells

EC and VSMC were enzymatically dissociated from arteries as previously described (Mendoza et al., 2010; Zhang et al., 2012). In brief, artery segments were cleaned of surrounding fat and connective tissue. Luminal blood was thoroughly flushed out by repeated perfusion with ice-cold HEPES buffer. Segments were cut into small rings and incubated for 10 min at room temperature in a low-Ca^{2+} dissociation solution consisting of (in mM) 140 NaCl, 5.0 KCl, 0.05 $CaCl_2$, 1.0 $MgSO_4$, 10 glucose, and 10 HEPES, with 0.1 % BSA (pH 7.4). The solution was carefully removed and vessel segments were incubated with papain (1.0 mg/mL) and dithiothreitol (0.5 mg/mL) in dissociation solution for 15 min at 37 °C, followed by incubation with collagenase (Sigma blend H; 1.0 mg/mL), trypsin inhibitor (1 mg/mL), and elastase (0.5 mg/mL) in dissociation solution for 15-30 min at 37ºC. All enzymes and chemicals were purchased from Sigma. Artery segments were then gently triturated to release cells contained in the vascular wall. The first few fractions collected during enzymatic dissociation were discarded to eliminate any remaining blood cells. All subsequent fractions were pooled and dissociated cells were washed twice in dissociation solution by centrifugation at 250 × g for 5 min. EC were separated from SMC by incubating the cell suspension with Dynabeads coated with anti-CD31 antibody (Thermo Scientific, Cat No. 11155D) for 60 minutes at 4 ºC, followed by bead pull-down using a magnet. Separated EC and SMC were stored on ice or at 4 ºC and used the same day for RNA extraction and reverse transcription as described below.

RNA extraction and reverse transcription-polymerase chain reaction

Freshly dissected human adipose (200-500 μm) and coronary (200-2000 μm) arteries were snap-frozen in liquid nitrogen and stored at -80 °C until use. In some vessels, the endothelium was removed by gentle scraping of the lumen with a metal wire. Total RNA was extracted using the RNeasy Fibrous Tissue Mini Kit (Qiagen) and cDNA was synthesized using SuperScript III

reverse transcriptase (Invitrogen), according to the manufacturer's instructions. 2-5 ng of cDNA was amplified in a Peltier thermal cycler (MJ Research, model PTC-200) using Platinum PCR Supermix (Invitrogen) and a 40-45 cycle touch-down protocol. Gene-specific primers were synthesized by Integrated DNA Technologies Inc. (Coralville, Iowa). Detailed sequence information is provided in Table 2. Two negative controls, without reverse transcription (RT-) and without template (H_2O), were amplified in parallel using TRPV1 primers. Human brain total RNA samples from a normal donor (Agilent Technologies, Santa Clara, CA) were included as a positive control since the brain tissue is known to express TRPV1 channels (Sawamura et al., 2017).

Quantitative PCR (qPCR) was performed using CFX96 C1000 Thermal Cycler (BioRad). The reactions were conducted in a 20 µL volume containing 10 µL 2x all-in-One SYBR Green qPCR mix (Qiagen), 1 µL (each for forward and reverse) of TRPV1/PECAM-1/SM22-specific primers, nuclease-free water and 2 µL of cDNA from pooled samples. cDNA was synthesized from EC and SMC RNA, derived from each patient and 10 ng of cDNA from each patient sample in duplicates was used for qPCR. Cycle threshold (Ct) values of products were determined using Bio-Rad CFX Manager 3.1 software (BioRad). For primer sequences, refer to Table 2. The thermal profile employed 1 cycle of initial denaturation at 95 ºC for 5 min, 40 cycles of denaturation at 95 ºC for 10 sec, annealing at 60 ºC for 30 sec and extension at 72 ºC for 15 sec. Melting curve analysis was performed immediately after the 40^{th} cycle at 72 to 95 ºC with 0.5 degree increments for 5 sec.

Preparation of membrane proteins

Freshly dissected human adipose (200-500 µm) and coronary (200-2000 µm) arteries were cleaned from the surrounding fat and connective tissue and placed in ice-cold HEPES buffer. Vessels were frozen in liquid nitrogen if not used immediately. Arterial membrane proteins were prepared with a differential centrifugation protocol as described previously (Zhang et al., 2001; Nishijima et al., 2016) All procedures were performed on ice or at 4^oC. Briefly, vascular tissues were homogenized with a Tenbroeck glass homogenizer in 2-5 volumes of an ice-cold homogenization buffer (20 mM HEPES pH 7.4, 250 mM sucrose, 1 mM EDTA, supplemented with protease and phosphatase inhibitor cocktail) and sonicated every 10 seconds (x3) with 1-2 minute(s) interval on ice (Fisher Scientific Sonic Dismembrator model D100). The homogenates were centrifuged at 3,000 ×*g* for 10 minutes, the supernatants were transferred to a new tube and centrifuged at 10,000 ×*g* for 20 minutes, and the supernatants were then centrifuged at 100,000 ×*g* for 90 minutes (Beckman TLA-

100.3 rotor, 50,000 rpm). The pellets containing crude membrane fraction were re-solubilized in a detergent-containing extraction buffer containing (in mM) 25 Tris-HCl pH 7.4, 150 NaCl, 1 EDTA, 1 % NP40, 0.5 % sodium deoxycholate, and 5 % glycerol, supplemented with protease and phosphatase inhibitors. Protein samples were aliquoted, frozen in liquid N_2, and stored at −80 °C until use.

Immunoblotting

All immunoblotting and immunohistochemical staining procedures comply with recommendations detailed in the BJP editorial (Alexander et al., 2018). Protein samples (20 µg) were separated by SDS-PAGE on 10 % gels and transferred to polyvinylidene difluoride membranes. Membranes were blocked by 5% non-fat dry milk (NFDM) or bovine serum albumin (BSA) for 1 hour at room temperature and incubated overnight at 4 °C with a primary antibody against TRPV1 (sc-12498, Santa Cruz, goat polyclonal IgG); 1:500 dilution in TBST with 5 % NFDM or BSA. Blots were then washed with TBST prior to the addition of an HRP-conjugated rabbit anti-goat IgG secondary antibody (1:10,000 dilution in TBST with 5 % NFDM or BSA) for 1 hour at room temperature. Membranes were developed using the ECL Prime reagent (Amersham) and scanned using an EPSON scanner.

Immunofluorescence

Freshly dissected arteries were embedded in optimal cutting temperature (OCT) compound, frozen on dry-ice, and cut into 10-µm sections (Mendoza et al., 2010). Some tissue sections were stained with hematoxylin and eosin to confirm the intact vascular structure before further processing for immunofluorescence staining. Tissue sections were washed in PBS and blocked with 5 % normal rabbit serum in PBS containing 0.1 % Triton X-100. Sections were then probed with a polyclonal antibody against TRPV1 (1:200 dilution; sc-12498, Santa Cruz) overnight at 4 ºC, followed by secondary probing with an Alexafluor 568-conjugated rabbit anti-goat IgG antibody (1:400 dilution) for 1 h at room temperature. After several washes with PBS, sections were counterstained with DAPI, a fluorescence nuclear probe and mounted in SlowFade antifade medium (Invitrogen). Images were immediately captured using a confocal fluorescence microscope (model A1-R, Nikon) with a 60× (NA 1.40) oil objective**.**

Measurement of intracellular Ca^{2+} concentration

Freshly dissected human adipose resistance arteries (250-500 µm) were partially denuded by gently rubbing with a metal wire, cut open along their longitudinal axis and pinned onto a Sylgard -coated block (Mendoza et al., 2010). Arterioles were then loaded with the calcium indicator fura-2 AM (Molecular Probes, Life Technology) by incubating in Krebs physiological saline solution (PSS) (in mM; NaCl 123, KCl 4.7, $MgSO_4$ 1.2, $CaCl_2$ 2.5, $NaHCO_3$ 19, KH_2PO_4 1.2, EDTA 0.026, and glucose 11) containing fura-2 AM (5 µM) for 60 minutes in 5 % CO_2 cell incubator at 37 °C. Post incubation, arteries were washed three times with HEPES-HBSS buffer (in mM; NaCl 123, KCl 5.4, $CaCl_2.2H_2O$ 1.6, $MgCl_2.6H_2O$ 0.5, $MgSO_4.7H_2O$ 0.4, $NaHCO_3$ 4.2, $Na_2HPO_4.7H_2O$ 0.3, KH_2PO_4 0.4, EDTA 0.026, HEPES 20, Glucose 5.5, pH 7.4) and mounted on the stage of a fluorescence microscope. MetaFluor software (Molecular Devices) was used to record and analyze the emitted fura-2 fluorescence at 510 nm after alternative excitation at 340 and 380 nm respectively. 30 areas were randomly selected in each magnifying field and fluorescence images were captured every 3 s for 20 to 30 minutes. Background fluorescence was subtracted before calculating the ratio of the emitted fluorescence intensities after alternate excitation at 340 nm and 380 nm respectively (F340/F380). Experiments were performed at 27 ^{o} C. Data were expressed as mean F340/F380 ratios ± SEM obtained in response to bath application of cumulative concentrations of capsaicin (100 nM-1 µM), in the absence or presence of SB366791 (1 µM).

Isometric tension recording

Arterioles (150-250 µm) were isolated from fresh human adipose tissues and cut into 1.5 mm segments. The segments were threaded on two stainless steel wires (25 or 40 µm diameter), mounted in a multi-chamber wire myograph (DMT model 610M) and equilibrated at 37 °C for 30 min in Krebs PSS, continuously gassed with a mixture of 21 % O_2, 5 % CO_2 and 74 % N_2 to maintain pH 7.4. The resting tension was set at 0.5-1 mN. This normalization method produces near maximal and reproducible contraction to high potassium physiological saline solution (high-K^+ PSS) based on previous length-tension studies and results in the lumen diameter that the artery would approximately have when cannulated under a transluminal pressure of 60 mmHg. Arterioles were then stimulated once with high-K^+ PSS (final K^+ 80 mM, NaCl was substituted with KCl of equal molar concentration) for 1-2 min before the initiation of experimental protocols. Where indicated, the endothelium was removed by gently rubbing the intimal layer of the arteriole with a

human hair. The endothelium was considered intact if acetylcholine (10 µmol/L) caused >80 % relaxation of ET-1-constricted vessels and effectively denuded if acetylcholine induced <10 % relaxation. At the end of each experiment, papaverine (100 µmol/L), an endothelium-independent vasodilator, was added on high-K^+ PSS (80 mM K^+)-preconstricted arterioles to determine maximal dilation and ensure optimal vascular smooth muscle function. The initial response to 80 mM K^+ before papaverine was used to define the maximum contraction.

Changes in vessel tension from resting tension were measured in non-preconstricted and ET-1 (0.1-0.5 nM) preconstricted (5-20 % preconstriction) arterioles in response to cumulative concentrations of capsaicin (1 nM - 1 µM), added to the vessel bath in the absence or presence of 30 min preincubation with the TRPV1-selective antagonist SB366791 (1-3 µM). Data were expressed as mean percent maximum contraction ± SEM. Percent maximum contraction was calculated using the following equations:

1. Percent maximum contraction in the absence of ET-1 = [{(tension developed with test compound) – (baseline tension)}/{(tension developed with 80 mM K^+) – (baseline tension)}]*100
2. Percent maximum contraction in the presence of ET-1 = [{(tension developed with test compound) – (tension developed with ET-1)}/{(tension developed with 80 mM K^+) – (baseline tension)}]*100

Cannulated arteriolar preparation

Arterioles (100-250 µm) were carefully dissected from fresh human adipose or coronary tissues or rat mesenteric tissue. Vessels were cannulated with two glass micropipettes for continuous measurements of internal diameter with a video system as previously described (Nishijima et al., 2016) or with a commercial pressure myograph system (model 110P, Danish Myo Technology A/S, Denmark). Vessels were pressurized to an intraluminal pressure of 60 mmHg under no-flow conditions and equilibrated for 1 hour at 37 °C in Krebs PSS continuously gassed with a mixture of 21 % O_2, 5 % CO_2 and 74 % N_2 to maintain pH 7.4.

Changes in luminal diameter from baseline diameter were measured in non-preconstricted and ET-1 (0.1-0.5 nmol/L) preconstricted (20-30 % preconstriction) arterioles in response to bath application of cumulative concentrations of capsaicin (1 nM - 1 µM), in the absence or presence of 20-30 min preincubation with the TRPV1-selective antagonist SB366791 (1 µM). Luminal

diameters were recorded after contraction/dilation reached steady state for each concentration of capsaicin. In some arterioles, the endothelium was mechanically removed by perfusing 3-5 mL of air through the lumen. The endothelium was considered intact if acetylcholine (10 µM) caused >80 % relaxation of ET-1-constricted vessels and effectively denuded if acetylcholine induced <10 % relaxation. At the end of each experiment, papaverine (100 µM), an endothelium-independent vasodilator, was added to the vessel bath to ensure optimal smooth muscle function. Unless otherwise stated, experiments were performed on endothelium-intact arterioles. Percent maximum contraction/dilation were calculated using the following equations:

1. Percent maximum dilation = [{(Luminal diameter with test compound) – (Luminal diameter with ET-1)}/{(Maximum luminal diameter) – (Luminal diameter with ET-1)}]*100
2. Percent maximum contraction in the absence of ET-1 = [{(Baseline luminal diameter) – (Luminal diameter with test compound)}/{(Baseline luminal diameter) – (Minimum luminal diameter)}]*100
3. Percent maximum contraction in the presence of ET-1 = [{(Luminal diameter after ET-1) – (Luminal diameter with test compound)}/{(Baseline luminal diameter) – (Minimum luminal diameter)}]*100

Some arterioles were preconstricted with high-K^+ PSS) (20-40 mM) or phenylephrine (200-1000 nM) (20-30 % preconstriction) before measuring vasomotor responses with capsaicin. Some non-preconstricted or ET-1 preconstricted arterioles were preincubated for 60 minutes with the PKC-selective antagonist GF109203X prior to measuring vasomotor responses with capsaicin.

Experimental Design

As recommended in the BJP editorial on experimental design and analysis in pharmacology (Curtis et al., 2018), studies were designed to facilitate pairwise comparisons between treatment groups of equal sizes, using randomization and blinded analysis. Group sizes were estimated based on pilot studies where approximately 5-10 vessels (1 vessel/patient) were required per group to detect a 20 % difference between groups, with an alpha (α) error of 0.05 and a power of 0.80. Paired studies were used unless otherwise indicated, where control/treatment group data were generated from the same vessel in cannulated preparations, and from either the same or as appropriate parallel segments of the same vessel in wire myograph preparations. For figures 2B and 5D, data also

include vessels isolated from different subjects resulting in unequal group sizes. Declared group sizes represent the number of independent values (one data point per patient) and all statistical analyses were performed using such independent values (technical replicates were not considered independent values).

Data and Statistical Analysis

All data are presented as means ± SEM and all analyses were conducted using the statistical programs in SigmaPlot, version 12.5. Data comparing capsaicin concentration-response curves between treatments were tested for statistical significance using two-factor (factor 1: capsaicin concentration; factor 2: presence or absence of an intact endothelium/inhibitors/ET-1/phenylephrine/High-K^+ PSS) repeated measures analysis of variance (ANOVA), whereas, data comparing responses at different concentrations or responses between different treatments were analyzed using one-factor ANOVA (factor: capsaicin concentration or treated vs untreated). After ANOVA, the Holm-Sidak post hoc test was run on datasets to facilitate multiple comparisons between individual datapoints from different groups. All data subjected to ANOVA and post hoc analyses passed the 'Shapiro-Wilk Normality Test', thus confirming their gaussian distribution and parametric nature. No significant variance inhomogeneity was detected as confirmed by an 'Equal Variance Test' built into the software. Curve fitting was performed using the ligand binding sigmoidal dose-response function. Only one level of probability (P) value was used throughout the manuscript to determine statistical significance between group means and P value < 0.05 was considered statistically significant. The data and statistical analyses comply with the recommendations on experimental design and analysis in pharmacology (Curtis et al., 2018).

Materials

Capsaicin, ET-1 and phenylephrine were obtained from Sigma. SB366791 and GF109203X were obtained from Tocris Bioscience. All other chemicals were purchased from Sigma. Capsaicin and SB366791 stock solutions (1000X or higher concentration) were prepared in 95 % ethanol, phenylephrine stock was prepared in distilled water, ET-1 stock was prepared in saline solution supplemented with 1 % BSA. Final solutions, serial dilutions were freshly prepared in distilled water.

Compliance with requirements for studies using animals

Male, 2-4 months old, Wistar Kyoto (WKY) rats were used in this study. Rats were housed in our environmentally controlled animal rooms (temperature setpoint at 21 ^{o} C +/- 1 degrees, and humidity setpoint at 45 %, range 30-70 %) under a 12/12-h day/night cycle and had access to food and water ad libitum. Rats were housed two/cage (cage model Allentown 40 individually ventilated cage with hardwood chip bedding). All animals were euthanized with pentobarbital (100 mg/kg, i.p.) and the third-order branches of the superior mesenteric artery were dissected for vessel reactivity. All animal studies were conducted in compliance with MCW's Institutional Animal Care and Use Committee guidelines, the ARRIVE guidelines (Kilkenny et al., 2010) and with the recommendations made by the *British Journal of Pharmacology* (BJP).

Results

TRPV1 expression in human arteries

We first examined if TRPV1 channels are expressed in the human vasculature at the transcript and protein level. Using RT-PCR, TRPV1 transcripts were detected in endothelium-intact coronary and adipose arteries, endothelium-denuded arteries and the human brain (included as positive control) (Fig. 1A). Using qRT-PCR, TRPV1 transcripts were also detected in isolated human EC and VSMC (Fig. 1B, C). The endothelial-specific marker, PECAM-1 was highly expressed in isolated EC preparation and was undetectable in isolated VSMC preparation. The vascular smooth muscle-specific marker,SM22 showed 4-fold higher expression in VSMC than in EC preparation. This demonstrated purity of the isolated cellular preparations. Using immunoblotting, TRPV1 proteins were detected in membrane protein preparations of human coronary and adipose arteries and in total protein lysates of HEK-293 cells transfected with the hTRPV1-mGFP fusion protein (~122 kDa band). No bands were detected in non-transfected HEK-293 protein lysates (Fig. 1D). Immunofluorescence localization revealed cell-type specific expression of TRPV1 (red fluorescence) on EC and VSMC of human adipose and coronary arteries with no staining in control sections exposed to fluorescently tagged secondary antibodies alone (Fig. 1E). Moreover, TRPV1 fluorescence colocalized with GFP fluorescence in hTRPV1-mGFP transfected HEK-293 cells with no staining in non-transfected cells (Fig. S1). This demonstrated the activity of the TRPV1 antibody (sc-12498, Santa Cruz) against human TRPV1. Together, these results indicate that TRPV1 is expressed in human coronary and adipose arteries, both in endothelial and vascular smooth muscle cells.

Vasomotor function of TRPV1 in human arterioles

To characterize the vasomotor function of TRPV1 in the human microvasculature, *ex-vivo* vascular reactivity studies were performed on freshly isolated HAA using isometric tension recording. Capsaicin was used to selectively activate vascular TRPV1 channels. Capsaicin (1 nM-1 µM) induced a concentration-dependent increase in arteriolar basal tension in endothelium-intact and endothelium-denuded HAA (Fig. 2A-B), which was significantly inhibited by preincubation of HAA with SB366791 (Fig. 4B, 5B). These results indicate that capsaicin induces vasoconstriction in human adipose arterioles and that this effect is largely endothelium independent. Although the

percentage constriction observed in endothelium-denuded arterioles was greater than that in endothelium-intact arterioles, the difference did not reach statistical significance. Consistent with findings from the human adipose vascular bed, capsaicin (1 nM-1 µM) also induced concentration-dependent constriction of human coronary arterioles (HCA) that were preconstricted with ET-1. This constriction was significantly inhibited by preincubation of HCA with SB366791 (1 µM) (Fig. S3, refer to Table 3 for data on vessel diameters). Due to limited availability of human coronary tissues, parallel studies assessing the effect of capsaicin on the basal tone of HCA were not conducted. In contrast to findings in human arterioles, capsaicin induced concentration-dependent vasodilation in rat small mesenteric arteries (Fig. S2). These rat mesenteric data are consistent with previous reports (Poblete et al., 2005; Yang et al., 2010) and demonstrate reproducibility of our experimental protocol.

Mechanism of TRPV1-mediated vasoconstriction in human adipose small arteries

To further elucidate the mechanism of capsaicin-induced constriction in human small adipose arteries, we assessed intracellular Ca^{2+} concentration in human VSMC *in situ* using ratiometric calcium imaging. In human small adipose arteries (250-500 µm luminal diameter) largely denuded of endothelial cells, capsaicin (100 nM-1 µM) induced a concentration-dependent increase in $[Ca^{2+}]_i$ in VSMC *in situ* (observed indirectly as an increase in green fluorescence and in F340/380 ratio), which was subsequently inhibited by addition of SB366791 (1 µM) to the vessel bath (Fig. 3A-B). Averaged data indicate that capsaicin (500 nM–1 µM) induced a significant increase in $[Ca^{2+}]_i$ in human VSMC, which was significantly inhibited by SB366791 (1 µM) (Fig. 3C). These data are consistent with vasoconstriction responses described above (Fig. 2) and further support a vasoconstrictive role for VSMC TRPV1 channels in the human vasculature.

Potentiation of TRPV1-mediated vasoconstriction by ET-1

Given that ET-1 and TRPV1 both exert arteriolar vasoconstriction and are independently associated with the pathophysiology of vasospasm (Akçay et al., 2009; Saitoh et al., 2009, 2015; Boddhula et al., 2018), we sought to investigate the relationship between their vasomotor functions and hypothesized that ET-1 modulates the vasomotor function of vascular TRPV1 channels in the human microcirculation. Indeed, unpaired studies (control and treatment group data were collected from arterioles of the same/different human subjects) suggest that TRPV1 vasomotor function can

be modulated by ET-1. As indicated in Fig. 4A-C, constriction responses to capsaicin were measured in endothelium intact HAA (100-250 µm) with/without ET-1 preconstriction. Preconstriction with ET-1 significantly potentiated capsaicin-induced constriction of endothelium-intact HAA as compared to non-preconstricted HAA (Fig. 4A-C). This potentiation response was significantly inhibited by preincubation of ET-1 preconstricted HAA with SB366791 (Fig. 4C). These results were further confirmed in paired studies (control and treatment group data were collected from arterioles of the same human subjects), conducted using wire and pressure myography. In paired studies, similar potentiation was observed in ET-1 preconstricted HAA as compared to non-preconstricted HAA (Fig. 4D, 6A, Table 3), although the extent of this potentiation was reduced due to greater ET-1 preconstriction in cannulated arterioles. Constriction response of HAA to escalating concentrations of ET-1 was studied as control. ET-1, in the absence of capsaicin, induced concentration-dependent constriction of HAA (Fig. S4) with potency consistent with recently published data in human gluteal biopsy adipose arterioles (Ford et al., 2018).

To delineate the contribution of vascular smooth muscle versus endothelial TRPV1 channels to ET-1-induced potentiation of capsaicin-evoked constriction, the endothelial layer was removed in some HAA before studying the potentiation response. Preconstriction with ET-1 slightly potentiated capsaicin-induced constriction of endothelium-denuded HAA (Fig. 5C) as compared to non-preconstricted, endothelium-denuded HAA (Fig. 5B), but failed to reach statistical significance. This potentiation response was significantly inhibited by preincubation of ET-1 preconstricted HAA with SB366791 (Fig. 5C). No significant differences in capsaicin-evoked constriction were observed between endothelium-intact and endothelium-denuded, ET-1 preconstricted HAA (Fig. 5D). These data indicate that most of ET-1-induced potentiation of capsaicin-evoked constriction is mediated through its effect on vascular smooth muscle cells.

Lack of significant potentiation of TRPV1-mediated vasoconstriction by high extracellular potassium and phenylephrine

To test if TRPV1-mediated vasoconstriction is specifically modulated by ET-1, endothelium-intact HAA were preconstricted either by depolarizing VSMC membrane with high-K^+ PSS or by activation of α-adrenergic receptors with phenylephrine, before measuring constriction responses to capsaicin. This study was conducted on cannulated arterioles in a pressure myograph setup.

Preconstriction with high-K^+ PSS (20-40 mM) or phenylephrine (200-1000 nM) did not potentiate capsaicin-induced constriction of endothelium-intact HAA as compared to non-preconstricted HAA (Fig. 6B-C, Table 3).Interestingly, the constriction response in high-K^+ PSS/phenylephrine preconstricted arterioles strongly plateaued at 1 μM capsaicin (saturating concentration) and was significantly smaller than that in non-preconstricted (control) arterioles at 1 μM capsaicin. These data suggest that TRPV1-mediated vasoconstriction is specifically enhanced by ET-1 but not by other vasoconstrictive stimuli such as high-K^+-PSS or phenylephrine.

PKC in TRPV1-mediated vasoconstriction and its potentiation by ET-1

To elucidate the mechanism of ET-1-induced potentiation of TRPV1-mediated vasoconstriction, we investigated the involvement of PKC in this potentiation response. Endothelium-intact HAA were preconstricted with ET-1 in the absence or presence of the PKC-selective antagonist GF109203X (1 μM), prior to measuring constriction responses to capsaicin. The same protocol was repeated on non-preconstricted, endothelium-intact HAA to determine if PKC activity regulated TRPV1 vasomotor function at baseline tone. Preincubation of HAA with GF109203X significantly inhibited potentiation of capsaicin-induced constriction by ET-1 (Fig. 7B, Table 3). Interestingly, GF109203X also significantly inhibited capsaicin-induced constriction of non-preconstricted HAA (Fig. 7A, Table 3). These results indicate that ET-1-induced potentiation of capsaicin-evoked constriction is partly mediated by PKC activity.

Discussion

To our knowledge, the present study is the first study to systematically characterize the expression and vasomotor function of TRPV1 channels in the human microcirculation and examine modulation of their vasomotor function by ET-1. The major findings of this study are as follows: first, TRPV1 channels are expressed in human resistance arteries of the adipose and coronary vascular beds, in both the endothelial and the smooth muscle layers. Second, activation of vascular TRPV1 channels with capsaicin induces vasoconstriction of HAA and HCA. This vasoconstriction is mediated by VSMC TRPV1 activation without significant contribution of endothelial TRPV1. Third, preconstriction with ET-1 but not high-K^+ PSS or phenylephrine potentiates capsaicin-induced constriction of HAA. This potentiation is mediated by the modulation of VSMC TRPV1 function by ET-1 without significant modulation of endothelial TRPV1 function. Fourth, ET-1-induced potentiation of capsaicin-induced constriction is partly mediated by PKC activity.

Role of vascular smooth muscle TRPV1 in regulation of vascular tone

Although it was suggested earlier that TRPV1-mediated vasoconstriction could be mediated by endothelin (Szolcsanyi et al., 2001) or substance P (Scotland et al., 2004) release from perivascular nerve endings, substantial evidence exists in support of a role for VSMC TRPV1 channels in arteriolar vasoconstriction. *In vivo,* TRPV1 activation with capsaicin leads to increases in rat hindlimb vascular resistance (Kark et al., 2008). Consistently, *in vitro,* capsaicin causes significant endothelium-independent and non-neuronal vasoconstriction of skeletal muscle arterioles (Lizanecz et al., 2006; Kark et al., 2008; Czikora et al., 2012), mesenteric arteries (Pórszász et al., 2002) and auricular arterioles (Cavanaugh et al., 2011). Interestingly, in canine coronary arteries, direct activation of TRPV1 with capsaicin is not enough to stimulate vasoconstriction but requires preconstriction with the prostaglandin $F_{2\alpha}$ ($PGF_{2\alpha}$) to unmask capsaicin's vasoconstrictive effect (Hiett et al., 2014).

We extend these findings to the human vasculature and demonstrate that TRPV1 channels are expressed and functional in the human coronary and adipose vasculatures. Upon activation of vascular TRPV1 channels with capsaicin, HAA undergo sustained vasoconstriction, which can be attributed to TRPV1-mediated Ca^{2+} increase in VSMC and subsequent activation of their contractile apparatus. Although the source of this Ca^{2+} wasn't determined, capsaicin-stimulated

intracellular Ca^{2+} increase was largely inhibited by SB366791, which only has minimal (insignificant) antagonistic activity against voltage-gated Ca^{2+} channels (VGCC) (Gunthorpe et al., 2004). These results indicate that TRPV1 is likely the main mediator of such Ca^{2+} increase. However, given that TRPV1-mediated Ca^{2+} influx may depolarize the VSMC membrane, we cannot exclude the possibility that such depolarization could subsequently activate VGCC to contribute to the Ca^{2+} response. In a similar manner, potential Ca^{2+} release from intracellular Ca^{2+} stores in response to TRPV1-mediated Ca^{2+} entry (via Ca^{2+}-induced Ca^{2+} release) cannot be excluded either and could be pursued in future studies. Moreover, capsaicin-induced constriction responses are consistent between the wire and pressure myograph vessel setups, which further strengthen our findings. Endothelium removal did not significantly augment or inhibit capsaicin-induced vasoconstriction, suggesting that EC TRPV1 channels do not contribute to this response. The magnitude of constriction in endothelium-denuded HAA tends to be greater than that in endothelium-intact HAA, which is likely due to the basal release of endothelial relaxing factors in these arterioles. Although TRPV1 expression was detected on human endothelial cells, current data do not support a functional role for endothelial TRPV1 channels in capsaicin-induced vascular effects in the human vasculature and it remains to be determined whether endothelial TRPV1 activation with capsaicin can stimulate the release of vasodilatory factors.

Our findings are consistent with recent reports demonstrating TRPV1-mediated vasoconstriction but are in stark contrast to other reports that show an endothelium-dependent vasodilatory role for TRPV1 in other vascular beds and species. For example, in the mouse coronary and mesenteric vascular beds, endothelial TRPV1 channels possess a vasodilatory role (Yang et al., 2010; Guarini et al., 2012) and increase coronary blood flow upon activation. Similarly, in the human skeletal muscle vascular bed, endothelial TRPV1 activation with capsaicin attenuates α-receptor-mediated vasocontraction and enhances acetylcholine-induced vasorelaxation (Ives et al., 2017); however, these studies were performed on large feed arteries (0.6-0.7 mm internal diameter) and were not extended to the microcirculation. Thus, our findings accentuate the inherent differences in TRPV1 protein function across different vascular beds and species and provide new translational insight into the vasomotor function of TRPV1 in the human microvasculature.

Modulation of TRPV1 vasomotor function and arteriolar hypercontractility

TRP channel activity and sensitivity to ligands is enhanced by interactions between receptor-mediated and other signaling modalities within cells. For example, coactivation of inositol 1,4,5-

trisphosphate and vasopressin receptors exert synergistic stimulatory effects on vascular TRPC6 channels (Maruyama et al., 2006). Also, TRPC6 channel phosphorylation by protein kinase A (PKA) amplifies the activating effects of angiotensin-II on TRPC6 (Nishioka et al., 2011). In the canine coronary circulation, the vasoconstrictive role of TRPV1 is unmasked by preconstriction of arteries with the vasoconstrictive autacoid $PGF_{2\alpha}$. Consistently, the intracellular Ca^{2+} response to capsaicin is also dramatically enhanced by $PGF_{2\alpha}$ in isolated coronary artery smooth muscle cells (Hiett et al., 2014). These data uncover the modulatory action of $PGF_{2\alpha}$ on TRPV1 vasomotor function and show that such modulation can enhance vascular smooth muscle contractility, thus implicating TRPV1 channels in the pathogenesis of coronary vasospasm.

We show that capsaicin-induced constriction is significantly enhanced in HAA that are preconstricted with ET-1 as compared to non-preconstricted, control HAA, suggesting that ET-1 sensitizes vascular TRPV1 channels to capsaicin. Endothelium removal did not significantly alter capsaicin-induced constriction in ET-1 preconstricted HAA, indicating that endothelial TRPV1 channels do not significantly contribute to the ET-1-induced potentiation response and that ET-1-induced sensitization of VSMC TRPV1 predominantly mediates this response. Furthermore, the specificity of ET-1-induced potentiation response was determined by preconstricting HAA with two other vasoconstrictive stimuli, high-K^+ PSS and phenylephrine. Neither high-K^+ PSS nor phenylephrine potentiated capsaicin-induced constriction significantly, suggesting that VSMC TRPV1 channels are not sensitized downstream of non-receptor-mediated activation by high-K^+ PSS or α-adrenergic receptor activation by phenylephrine. These data indicate that signaling initiated by ET-1 downstream of ET-1 receptors' activation on VSMC specifically modulates TRPV1 vasomotor function in HAA.

Lastly, the mechanism of ET-1-induced potentiation response was investigated using PKC-selective pharmacology. A role for PKC in $PGF_{2\alpha}$-induced sensitization of TRPV1 to capsaicin has previously been demonstrated in the canine coronary vasculature (Hiett et al., 2014). In rodent skeletal muscle arteries, its role in desensitization of VSMC TRPV1 channels by anandamide has also been reported (Lizanecz et al., 2006). In our study, inhibition of PKC activity significantly inhibited the ET-1-induced potentiation response, suggesting that ET-1-induced sensitization of VSMC TRPV1 channels partly occurs through channel phosphorylation mediated by PKC (schematic presented in graphical abstract). However, the exact contribution of PKC in ET-1-induced sensitization remains unclear and needs to be explored in future studies along with PKC-

independent mechanisms of such ET-1-induced sensitization. Surprisingly, inhibition of PKC activity also significantly inhibited capsaicin-induced constriction in non-preconstricted HAA, suggesting that TRPV1 channels exist in a phosphorylated state at resting tone and that PKC-mediated channel phosphorylation regulates channel activation with capsaicin. These data also shed light on the ET-1 independent sensitization action of PKC on TRPV1, which remains to be explored. Given that ET-1 potentiated capsaicin-induced constriction even when PKC was inhibited clearly suggests the involvement of other mechanisms of ET-1 stimulated TRPV1 sensitization (eg. TRPV1 phosphorylation by other cellular kinases), which were beyond the scope of this study and hence not explored.

ET-1-induced potentiation of TRPV1-mediated constriction could be mediated by a) sensitization of VSMC TRPV1 to capsaicin or b) sensitization of the contractile apparatus, specifically myosin light chain (MLC) to TRPV1-mediated Ca^{2+} influx. Both ET-1 and phenylephrine activate phospholipase C-linked G_q-coupled receptors on VSMC and elicit sustained vasoconstriction through Ca^{2+}-dependent and independent signaling pathways (Kuo and Ehrlich, 2015; Brozovich et al., 2016). Since potentiation of capsaicin-induced constriction is only observed with ET-1 and not with phenylephrine, it is unlikely that ET-1 potentiates TRPV1-mediated vasoconstriction by sensitizing MLC to calcium but instead by sensitizing TRPV1 to capsaicin. Such sensitization could possibly contribute to arteriolar hypercontractility through one of the following mechanisms which remain to be explored. It could either lower their threshold for activation with capsaicin, in which case, vasoconstriction would be observed with a lower concentration of capsaicin in ET-1 sensitized arterioles as compared to control arterioles. Alternatively, it could enhance the number of Ca^{2+} ions passing through TRPV1 at any given capsaicin concentration by reducing the rate of channel inactivation and promoting the open state of the channel, resulting in a larger Ca^{2+} influx and therefore constriction of a greater magnitude in ET-1 sensitized arterioles relative to control arterioles.

Study Limitations

We could not control for all patient characteristics since samples used in the study were obtained as surgical discards. The clinical profiles (demographics, medications, health history, etc.) of individuals within the non-CAD and CAD groups were not fully known. However, information regarding prior diagnosis of CAD and presence of risk factors was acquired. By defining our non-

CAD patient cohort as having one or no risk factor for CAD, we limited the extent to which non-CAD adipose samples were falsely classified as CAD. Human coronary tissues were all obtained from patients with CAD due to scarcity of coronary surgeries performed in non-CAD patients. Female subjects constituted approximately 80% of the patient cohort, thus introducing a degree of gender bias in this study. Our sample size for non-CAD males (n=8) remains underpowered to detect sex differences in vascular function within and between phenotypes. Vessels were isolated from different fat depots, but no significant differences in vascular responses to capsaicin were observed, as evident in previous publications where the mechanism of flow-induced dilation seems to be preserved across multiple vascular beds (Beyer et al., 2017). Although TRPV1-selective antagonists, well-documented in the literature were used to study TRPV1 vasomotor function, they may have non-specific or off-target effects. Current findings will be strengthened by complementary future studies utilizing a genetic knockdown (TRPV1-specific siRNA) approach.

Perspective on Clinical Implications

Although vasospasm is traditionally recognized as a disease of conduit epicardial arteries, characterized by an intense, focal and reversible vasoconstriction, microvascular spasm also represents a distinct clinical entity characterized by a diffuse increase in arteriolar sensitivity to vasoconstrictor stimuli (Konidala and Gutterman, 2004). Indeed, smooth muscle hypercontractility has been suggested as a plausible mechanism of coronary vasospasm under pathological conditions (Lamping Kathryn G., 2002; Hald and Alford, 2014; Saitoh et al., 2015). ET-1 is associated with the pathophysiology of coronary vasospasm. In a pig model of endothelial-injury-induced coronary vasospasm, ET-1 expression was upregulated and blockade of the ET_A receptor prevented development of spontaneous coronary artery spasms (Saitoh et al., 2009). Given the findings of the present study, it will be interesting to determine the role of vascular TRPV1 channels in smooth muscle hypercontractility, particularly in the human microcirculation.

In summary, we found that TRPV1 activation on vascular smooth muscle cells induces vasoconstriction of isolated human arterioles, consistent with recent clinical case reports of capsaicin-induced vasospasm in human coronary and cerebral arteries. Moreover, preconstriction with ET-1 potentiates such TRPV1-mediated vasoconstriction, mediated in part by PKC. Our findings uncover the role of TRPV1 channels in vascular smooth muscle hypercontractility and reveal a novel regulatory mechanism by ET-1, which may provide mechanistic insights into the

pathogenesis of vasospasm. Further studies are required to determine the role of TRPV1 and its interaction with ET-1 in microvascular hypercontractility under pathophysiological conditions such as coronary artery disease and acute myocardial infarction.

Author contributions

A.M.K., Y.N., Z.W., Y.X. and J.F. planned and performed the experiments. D.A.W. provided intellectual input or technical advice. A.M.K., Y.N., and D.X.Z. analyzed the data. A.M.K. and D.X.Z. conceived and designed the study. A.M.K wrote the manuscript. A.M.K., Y.N. and D.X.Z. critically reviewed and revised the manuscript.

Acknowledgements

We thank the following organizations for their assistance in providing human tissues for this study: Cardiovascular Surgery Associates of Milwaukee, Midwest Heart Surgery Institute, Wisconsin Heart Group, Wisconsin Donor Network, Wheaton Franciscan Healthcare's Elmbrook Memorial Hospital, St. Joseph's Hospital, Froedtert Memorial Lutheran Hospital and Aurora St. Luke's Medical Center. This work was supported by the National Heart, Lung and Blood Institute Grant RO1-HL 096647 (to D.X.Z.) and the American Heart Association Grant 18PRE34060242 (to A.M.K.) and generous gift from John B. and Judith A. Gardetto to the Children's Research Foundation (D.A.W.).

Conflict of Interest Statement

D.A.W is President of Platelet Targeted Therapeutics, LLC. Dr. Wilcox has equity interest and intellectual property rights in the company.

References

Akçay, A.B., Ozcan, T., Seyis, S., and Acele, A. (2009). Coronary vasospasm and acute myocardial infarction induced by a topical capsaicin patch. Turk Kardiyol. Dernegi Arsivi Turk Kardiyol. Derneginin Yayin Organidir *37*: 497–500.

Alexander, S.P.H., Roberts, R.E., Broughton, B.R.S., Sobey, C.G., George, C.H., Stanford, S.C., et al. (2018). Goals and practicalities of immunoblotting and immunohistochemistry: A guide for submission to the British Journal of Pharmacology. Br. J. Pharmacol. *175*: 407–411.

Baylie, R.L., and Brayden, J.E. (2011). TRPV channels and vascular function. Acta Physiol. Oxf. Engl. *203*: 99–116.

Beyer, A.M., Zinkevich, N., Miller, B., Liu, Y., Wittenburg, A.L., Mitchell, M., et al. (2017). Transition in the mechanism of flow-mediated dilation with aging and development of coronary artery disease. Basic Res. Cardiol. *112*: 5.

Boddhula, S.K., Boddhula, S., Gunasekaran, K., and Bischof, E. (2018). An unusual cause of thunderclap headache after eating the hottest pepper in the world - 'The Carolina Reaper'. BMJ Case Rep. *2018*:.

Bratz, I.N., Dick, G.M., Tune, J.D., Edwards, J.M., Neeb, Z.P., Dincer, U.D., et al. (2008). Impaired capsaicin-induced relaxation of coronary arteries in a porcine model of the metabolic syndrome. Am. J. Physiol. Heart Circ. Physiol. *294*: H2489-2496.

Brozovich, F.V., Nicholson, C.J., Degen, C.V., Gao, Y.Z., Aggarwal, M., and Morgan, K.G. (2016). Mechanisms of Vascular Smooth Muscle Contraction and the Basis for Pharmacologic Treatment of Smooth Muscle Disorders. Pharmacol. Rev. *68*: 476–532.

Bubolz, A.H., Mendoza, S.A., Zheng, X., Zinkevich, N.S., Li, R., Gutterman, D.D., et al. (2012). Activation of endothelial TRPV4 channels mediates flow-induced dilation in human coronary arterioles: role of Ca2+ entry and mitochondrial ROS signaling. Am. J. Physiol. Heart Circ. Physiol. *302*: H634-642.

Cavanaugh, D.J., Chesler, A.T., Jackson, A.C., Sigal, Y.M., Yamanaka, H., Grant, R., et al. (2011). Trpv1 reporter mice reveal highly restricted brain distribution and functional expression in arteriolar smooth muscle cells. J. Neurosci. Off. J. Soc. Neurosci. *31*: 5067–5077.

Curtis, M.J., Alexander, S., Cirino, G., Docherty, J.R., George, C.H., Giembycz, M.A., et al. (2018). Experimental design and analysis and their reporting II: updated and simplified guidance for authors and peer reviewers. Br. J. Pharmacol. *175*: 987–993.

Czikora, Á., Lizanecz, E., Bakó, P., Rutkai, I., Ruzsnavszky, F., Magyar, J., et al. (2012). Structure-activity relationships of vanilloid receptor agonists for arteriolar TRPV1. Br. J. Pharmacol. *165*: 1801–1812.

Earley, S., and Brayden, J.E. (2015). Transient Receptor Potential Channels in the Vasculature. Physiol. Rev. *95*: 645–690.

Fernandes, E.S., Fernandes, M.A., and Keeble, J.E. (2012). The functions of TRPA1 and TRPV1: moving away from sensory nerves. Br. J. Pharmacol. *166*: 510–521.

Ford, T.J., Rocchiccioli, P., Good, R., McEntegart, M., Eteiba, H., Watkins, S., et al. (2018). Systemic microvascular dysfunction in microvascular and vasospastic angina. Eur. Heart J. *39*: 4086–4097.

Gonzales, A.L., and Earley, S. (2013). Regulation of cerebral artery smooth muscle membrane potential by Ca^{2+}-activated cation channels. Microcirc. N. Y. N 1994 *20*: 337–347.

Gonzales, A.L., Garcia, Z.I., Amberg, G.C., and Earley, S. (2010). Pharmacological inhibition of TRPM4 hyperpolarizes vascular smooth muscle. Am. J. Physiol. Cell Physiol. *299*: C1195-1202.

Gonzales, A.L., Yang, Y., Sullivan, M.N., Sanders, L., Dabertrand, F., Hill-Eubanks, D.C., et al. (2014). A PLCγ1-dependent, force-sensitive signaling network in the myogenic constriction of cerebral arteries. Sci. Signal. *7*: ra49.

Guarini, G., Ohanyan, V.A., Kmetz, J.G., DelloStritto, D.J., Thoppil, R.J., Thodeti, C.K., et al. (2012). Disruption of TRPV1-mediated coupling of coronary blood flow to cardiac metabolism in diabetic mice: role of nitric oxide and BK channels. Am. J. Physiol. Heart Circ. Physiol. *303*: H216-223.

Gunthorpe, M.J., Rami, H.K., Jerman, J.C., Smart, D., Gill, C.H., Soffin, E.M., et al. (2004). Identification and characterisation of SB-366791, a potent and selective vanilloid receptor (VR1/TRPV1) antagonist. Neuropharmacology *46*: 133–149.

Hald, E.S., and Alford, P.W. (2014). Smooth muscle phenotype switching in blast traumatic brain injury-induced cerebral vasospasm. Transl. Stroke Res. *5*: 385–393.

Hartmannsgruber, V., Heyken, W.-T., Kacik, M., Kaistha, A., Grgic, I., Harteneck, C., et al. (2007). Arterial response to shear stress critically depends on endothelial TRPV4 expression. PloS One *2*: e827.

Hiett, S.C., Owen, M.K., Li, W., Chen, X., Riley, A., Noblet, J., et al. (2014). Mechanisms underlying capsaicin effects in canine coronary artery: implications for coronary spasm. Cardiovasc. Res. *103*: 607–618.

Inoue, R., Jensen, L.J., Shi, J., Morita, H., Nishida, M., Honda, A., et al. (2006). Transient receptor potential channels in cardiovascular function and disease. Circ. Res. *99*: 119–131.

Ives, S.J., Park, S.Y., Kwon, O.S., Gifford, J.R., Andtbacka, R.H.I., Hyngstrom, J.R., et al. (2017). TRPV1 channels in human skeletal muscle feed arteries: implications for vascular function. Exp. Physiol. *102*: 1245–1258.

Kark, T., Bagi, Z., Lizanecz, E., Pásztor, E.T., Erdei, N., Czikora, A., et al. (2008). Tissue-specific regulation of microvascular diameter: opposite functional roles of neuronal and smooth muscle located vanilloid receptor-1. Mol. Pharmacol. *73*: 1405–1412.

Kilkenny, C., Browne, W., Cuthill, I.C., Emerson, M., Altman, D.G., and NC3Rs Reporting Guidelines Working Group (2010). Animal research: reporting in vivo experiments: the ARRIVE guidelines. Br. J. Pharmacol. *160*: 1577–1579.

Konidala, S., and Gutterman, D.D. (2004). Coronary vasospasm and the regulation of coronary blood flow. Prog. Cardiovasc. Dis. *46*: 349–373.

Kuo, I.Y., and Ehrlich, B.E. (2015). Signaling in muscle contraction. Cold Spring Harb. Perspect. Biol. *7*: a006023.

Lamping Kathryn G. (2002). Enhanced Contractile Mechanisms in Vasospasm. Circulation *105*: 1520–1522.

Liu, D., Yang, D., He, H., Chen, X., Cao, T., Feng, X., et al. (2009). Increased transient receptor potential canonical type 3 channels in vasculature from hypertensive rats. Hypertens. Dallas Tex 1979 *53*: 70–76.

Lizanecz, E., Bagi, Z., Pásztor, E.T., Papp, Z., Edes, I., Kedei, N., et al. (2006). Phosphorylation-dependent desensitization by anandamide of vanilloid receptor-1 (TRPV1) function in rat skeletal muscle arterioles and in Chinese hamster ovary cells expressing TRPV1. Mol. Pharmacol. *69*: 1015–1023.

Maruyama, Y., Nakanishi, Y., Walsh, E.J., Wilson, D.P., Welsh, D.G., and Cole, W.C. (2006). Heteromultimeric TRPC6-TRPC7 channels contribute to arginine vasopressin-induced cation current of A7r5 vascular smooth muscle cells. Circ. Res. *98*: 1520–1527.

Mendoza, S.A., Fang, J., Gutterman, D.D., Wilcox, D.A., Bubolz, A.H., Li, R., et al. (2010). TRPV4-mediated endothelial Ca2+ influx and vasodilation in response to shear stress. Am. J. Physiol. - Heart Circ. Physiol. *298*: H466–H476.

Nishijima, Y., Cao, S., Chabowski, D.S., Korishettar, A., Ge, A., Zheng, X., et al. (2016). Contribution of KV1.5 Channel to H2O2-Induced Human Arteriolar Dilation and its Modulation by Coronary Artery Disease. Circ. Res.

Nishioka, K., Nishida, M., Ariyoshi, M., Jian, Z., Saiki, S., Hirano, M., et al. (2011). Cilostazol suppresses angiotensin II-induced vasoconstriction via protein kinase A-mediated phosphorylation of the transient receptor potential canonical 6 channel. Arterioscler. Thromb. Vasc. Biol. *31*: 2278–2286.

Peppiatt-Wildman, C.M., Albert, A.P., Saleh, S.N., and Large, W.A. (2007). Endothelin-1 activates a Ca2+-permeable cation channel with TRPC3 and TRPC7 properties in rabbit coronary artery myocytes. J. Physiol. *580*: 755–764.

Poblete, I.M., Orliac, M.L., Briones, R., Adler-Graschinsky, E., and Huidobro-Toro, J.P. (2005). Anandamide elicits an acute release of nitric oxide through endothelial TRPV1 receptor activation in the rat arterial mesenteric bed. J. Physiol. *568*: 539–551.

Pórszász, R., Porkoláb, A., Ferencz, A., Pataki, T., Szilvássy, Z., and Szolcsányi, J. (2002). Capsaicin-induced nonneural vasoconstriction in canine mesenteric arteries. Eur. J. Pharmacol. *441*: 173–175.

Saitoh, S., Takeishi, Y., and Maruyama, Y. (2015). MECHANISTIC INSIGHTS OF CORONARY VASOSPASM AND NEW THERAPEUTIC APPROACHES. Fukushima J. Med. Sci. *61*: 1–12.

Saitoh, S.-I., Matsumoto, K., Kamioka, M., Ohkawara, H., Kaneshiro, T., Ishibashi, T., et al. (2009). Novel pathway of endothelin-1 and reactive oxygen species in coronary vasospasm with endothelial dysfunction. Coron. Artery Dis. *20*: 400–408.

Sawamura, S., Shirakawa, H., Nakagawa, T., Mori, Y., and Kaneko, S. (2017). TRP Channels in the Brain: What Are They There For? In Neurobiology of TRP Channels, T.L.R. Emir, ed. (Boca Raton (FL): CRC Press/Taylor & Francis), p.

Scotland, R.S., Chauhan, S., Davis, C., De Felipe, C., Hunt, S., Kabir, J., et al. (2004). Vanilloid receptor TRPV1, sensory C-fibers, and vascular autoregulation: a novel mechanism involved in myogenic constriction. Circ. Res. *95*: 1027–1034.

Sogut, O., Kaya, H., Gokdemir, M.T., and Sezen, Y. (2012). Acute myocardial infarction and coronary vasospasm associated with the ingestion of cayenne pepper pills in a 25-year-old male. Int. J. Emerg. Med. *5*: 5.

Spassova, M.A., Hewavitharana, T., Xu, W., Soboloff, J., and Gill, D.L. (2006). A common mechanism underlies stretch activation and receptor activation of TRPC6 channels. Proc. Natl. Acad. Sci. U. S. A. *103*: 16586–16591.

Sullivan, M.N., and Earley, S. (2013). TRP channel Ca(2+) sparklets: fundamental signals underlying endothelium-dependent hyperpolarization. Am. J. Physiol. Cell Physiol. *305*: C999–C1008.

Szolcsanyi, J., Oroszi, G., Nemeth, J., Szilvassy, Z., Blasig, I.E., and Tosaki, A. (2001). Functional and biochemical evidence for capsaicin-induced neural endothelin release in isolated working rat heart. Eur. J. Pharmacol. *419*: 215–221.

Tóth, A., Boczán, J., Kedei, N., Lizanecz, E., Bagi, Z., Papp, Z., et al. (2005). Expression and distribution of vanilloid receptor 1 (TRPV1) in the adult rat brain. Brain Res. Mol. Brain Res. *135*: 162–168.

Wang, L.-H., Luo, M., Wang, Y., Galligan, J.J., and Wang, D.H. (2006). Impaired vasodilation in response to perivascular nerve stimulation in mesenteric arteries of TRPV1-null mutant mice. J. Hypertens. *24*: 2399–2408.

Yang, D., Luo, Z., Ma, S., Wong, W.T., Ma, L., Zhong, J., et al. (2010). Activation of TRPV1 by dietary capsaicin improves endothelium-dependent vasorelaxation and prevents hypertension. Cell Metab. *12*: 130–141.

Zhang, D.X., Borbouse, L., Gebremedhin, D., Mendoza, S.A., Zinkevich, N.S., Li, R., et al. (2012). H2O2-induced dilation in human coronary arterioles: role of protein kinase G dimerization and large-conductance Ca2+-activated K+ channel activation. Circ. Res. *110*: 471–480.

Zhang, D.X., Fryer, R.M., Hsu, A.K., Zou, A.P., Gross, G.J., Campbell, W.B., et al. (2001). Production and metabolism of ceramide in normal and ischemic-reperfused myocardium of rats. Basic Res. Cardiol. *96*: 267–274.

Figures and figure legends

Figure 1

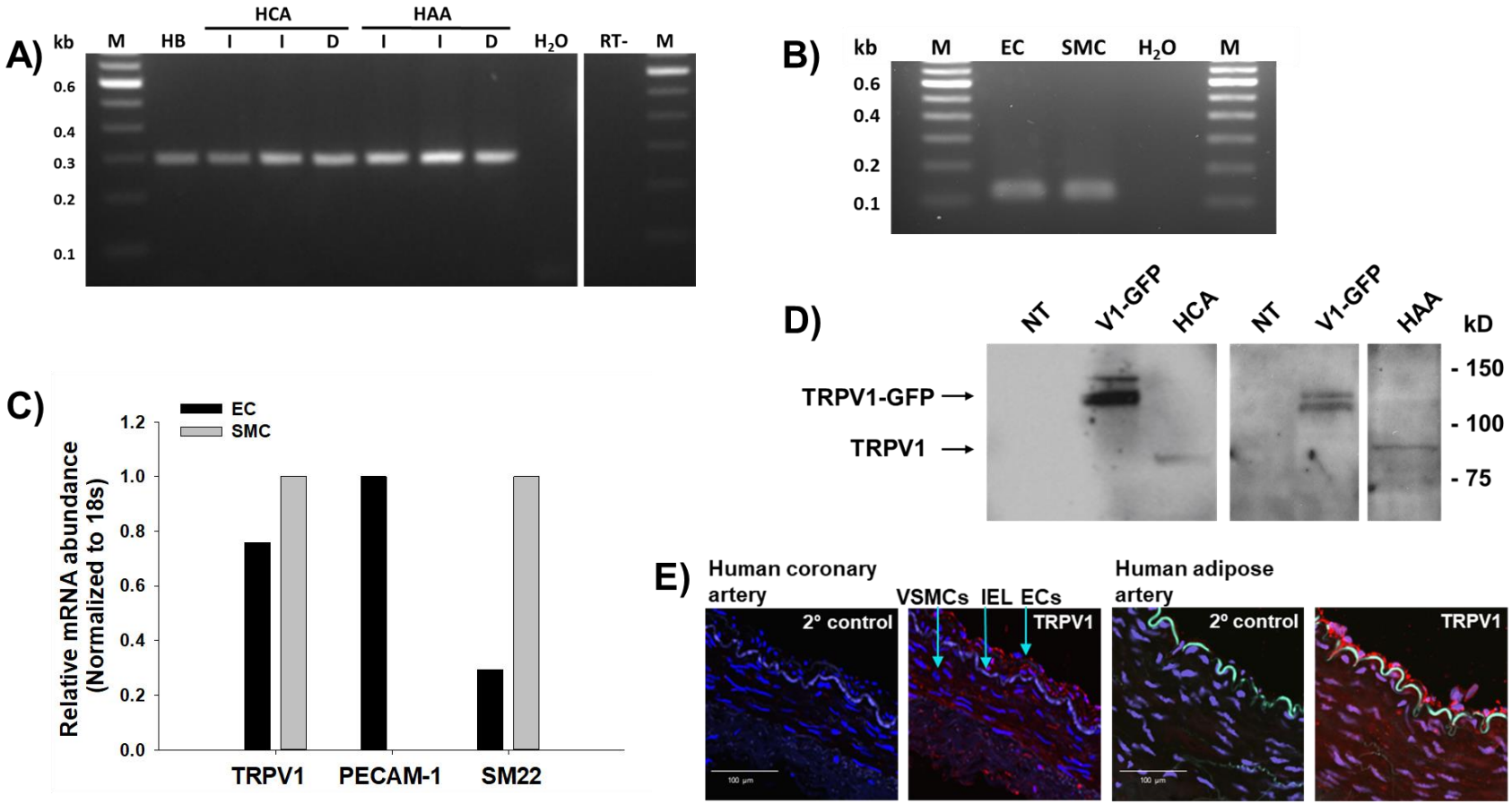

Figure 1. Expression of TRPV1 mRNA and proteins in human adipose and coronary arteries. A) Representative gel image of RT-PCR amplification products (Human TRPV1-295 bp) from human brain (HB), human coronary and adipose arteries (HCA and HAA; n=2 intact [I] and 1 denuded [D] artery each), without transcript (H_2O) and without reverse transcription (RT-) samples. RT- and marker (M) samples on the right are separated from HB, HCA, HAA and H_2O samples on the same gel by other unrelated samples, which are cropped out. **B)** Representative gel image of qRT-PCR amplification products (Human TRPV1-118 bp) from isolated human EC, SMC and H_2O samples. **C)** Relative TRPV1, PECAM-1 and SM22 mRNA abundance (normalized to 18s mRNA abundance) in isolated human EC and SMC by qRT-PCR (n=2 patients each). **D)** Representative immunoblot image showing TRPV1 protein expression (95 kD) in total protein lysates of non-transfected (NT), hTRPV1-mGFP-transfected (V1) HEK cells and membrane protein preparations of HCA (n=2 patients) and HAA (n=4 patients) **E)** Immunofluorescence localization of TRPV1 in human coronary and adipose arteries (Bar: 100 µm). Cell nuclei are stained in blue; Internal elastic lamina and TRPV1 are represented by green (autofluorescence) and red fluorescence respectively.

Figure 2

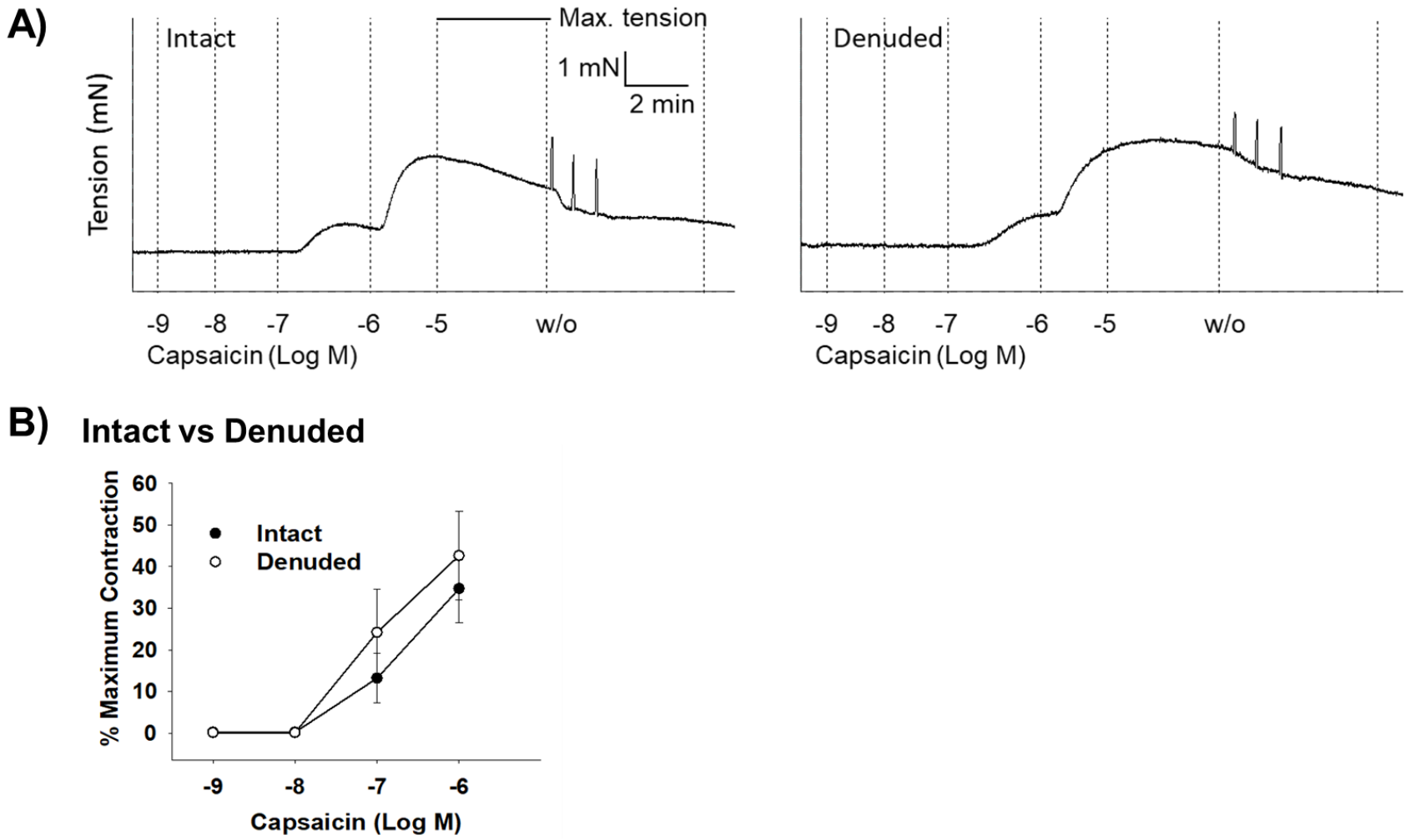
A)
Intact
Max. tension
1 mN
2 min
Tension (mN)
-9 -8 -7 -6 -5 w/o
Capsaicin (Log M)
Denuded
-9 -8 -7 -6 -5 w/o
Capsaicin (Log M)
B)
Intact vs Denuded
% Maximum Contraction
60
50
40
30
20
10
0
Intact
Denuded
-9 -8 -7 -6
Capsaicin (Log M)

Figure 2. Effect of capsaicin on tone of endothelium-intact and endothelium-denuded human adipose arterioles. A) Representative traces of tension (mN) generated in HAA following application of cumulative concentrations of capsaicin (1 nM-1 µM). **B)** Concentration response curves showing percent maximum constriction of endothelium-intact and endothelium-denuded HAA to cumulative concentrations of capsaicin (1 nM-1 µM). Capsaicin induced concentration-dependent vasoconstriction in both endothelium-intact (35 ± 8 % at 1 µM; n=11 vessels) and endothelium-denuded (43 ± 11 % at 1 µM; n=5 vessels) HAA. 1 vessel/patient.

Figure 3

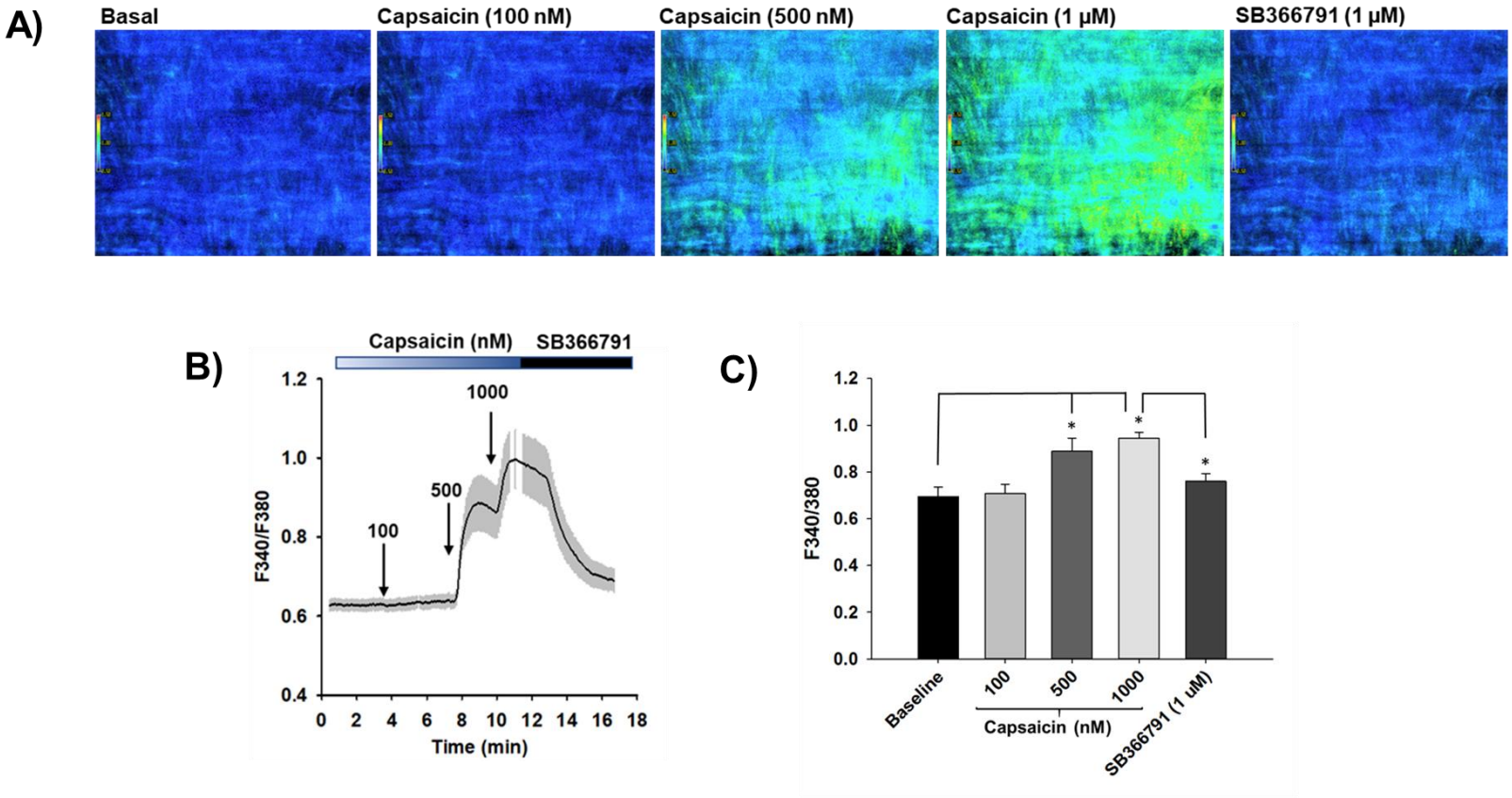
A)
Basal
Capsaicin (100 nM)
Capsaicin (500 nM)
Capsaicin (1 µM)
SB366791 (1 µM)
B)
Capsaicin (nM)
SB366791
1000
500
100
F340/F380
1.2
1.0
0.8
0.6
0.4
0 2 4 6 8 10 12 14 16 18
Time (min)
C)
F340/380
1.2
1.0
0.8
0.6
0.4
0.2
0.0
*
Baseline
100
500
1000
Capsaicin (nM)
SB366791 (1 uM)

Figure 3. Effect of capsaicin on $[Ca^{2+}]_i$ in human VSMC *in situ*. A, B) Representative images and trace showing changes in $[Ca^{2+}]_i$ in human VSMC *in situ* in response to bath application of cumulative concentrations of capsaicin (100 nM-1 µM), followed by SB366791 (1 µM). **C)** Summary data of changes in $[Ca^{2+}]_i$ with capsaicin. Capsaicin induced a concentration-dependent increase in VSMC $[Ca^{2+}]_i$ (increase in F340/F380 ratio from 0.7 at baseline to 0.9 at 1 µM capsaicin), which was significantly inhibited by SB366791 (Decrease in F340/F380 ratio from 0.9 at 1 µM capsaicin to 0.8 with 1 µM SB366791). **P*<0.05 by one-factor ANOVA; n=5 vessels, 1 vessel/patient.

Figure 4

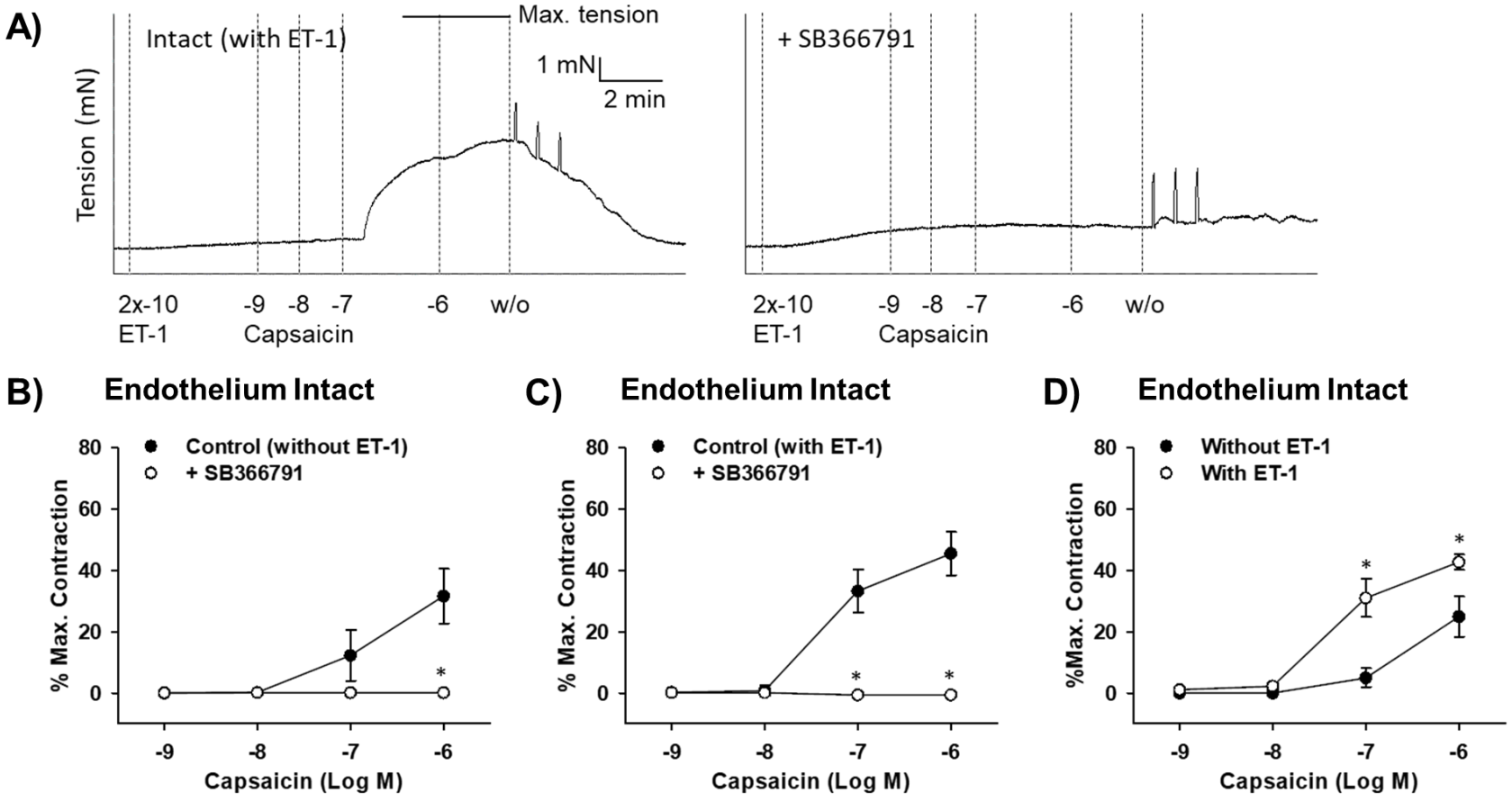
A)
Intact (with ET-1)
Max. tension
1 mN
2 min
Tension (mN)
2x-10
ET-1
-9 -8 -7
Capsaicin
-6
w/o
+ SB366791
2x-10
ET-1
-9 -8 -7
Capsaicin
-6
w/o
B)
Endothelium Intact
Control (without ET-1)
+ SB366791
% Max. Contraction
Capsaicin (Log M)
C)
Endothelium Intact
Control (with ET-1)
+ SB366791
% Max. Contraction
Capsaicin (Log M)
D)
Endothelium Intact
Without ET-1
With ET-1
%Max. Contraction
Capsaicin (Log M)

Figure 4. Effect of ET-1 preconstriction on capsaicin-induced constriction of endothelium-intact HAA. A) Representative wire myography traces of tension (mN) generated in ET-1 preconstricted, endothelium-intact HAA following application of cumulative concentrations of capsaicin (1 nM-1 µM), in the absence or presence of SB366791. Concentration response curves showing percent maximum constriction of unpaired, endothelium-intact, **B)** non-preconstricted and **C)** ET-1-preconstricted (11 ± 7 % preconstriction) HAA to cumulative concentrations of capsaicin (1 nM-1 µM). In non-preconstricted, endothelium-intact HAA, capsaicin induced concentration-dependent constriction (32 ± 9 % at 1 µM) which was significantly inhibited by preincubation with SB366791 (0.2 ± 0.1 %). Preconstriction with ET-1 significantly potentiated capsaicin-induced constriction of endothelium-intact HAA (33 ± 7 % at 100 nM capsaicin) as compared to non-preconstricted HAA (12 ± 8 % at 100 nM capsaicin). This potentiation response was significantly inhibited by preincubation of ET-1 preconstricted HAA with SB366791 (-1 ± 1 % at 100 nM capsaicin). **D)** Concentration response curves comparing percent maximum constriction of paired, endothelium-intact HAA to cumulative concentrations of capsaicin (1 nM-1 µM) between non-preconstricted and ET-1-preconstricted (7 ± 1 % preconstriction) arterioles, generated using wire myography. Preconstriction with ET-1 significantly potentiated capsaicin-induced constriction of paired, endothelium-intact HAA (43 ± 3 % at 1 µM) as compared to non-preconstricted HAA (25 ± 7 % at 1 µM). *P<0.05 by two-factor repeated measures ANOVA; n=6 vessels (Fig. 4B), n=9 vessels (Fig. 4C); n=6 vessels (Fig. 4D), 1 vessel/patient.

Figure 5

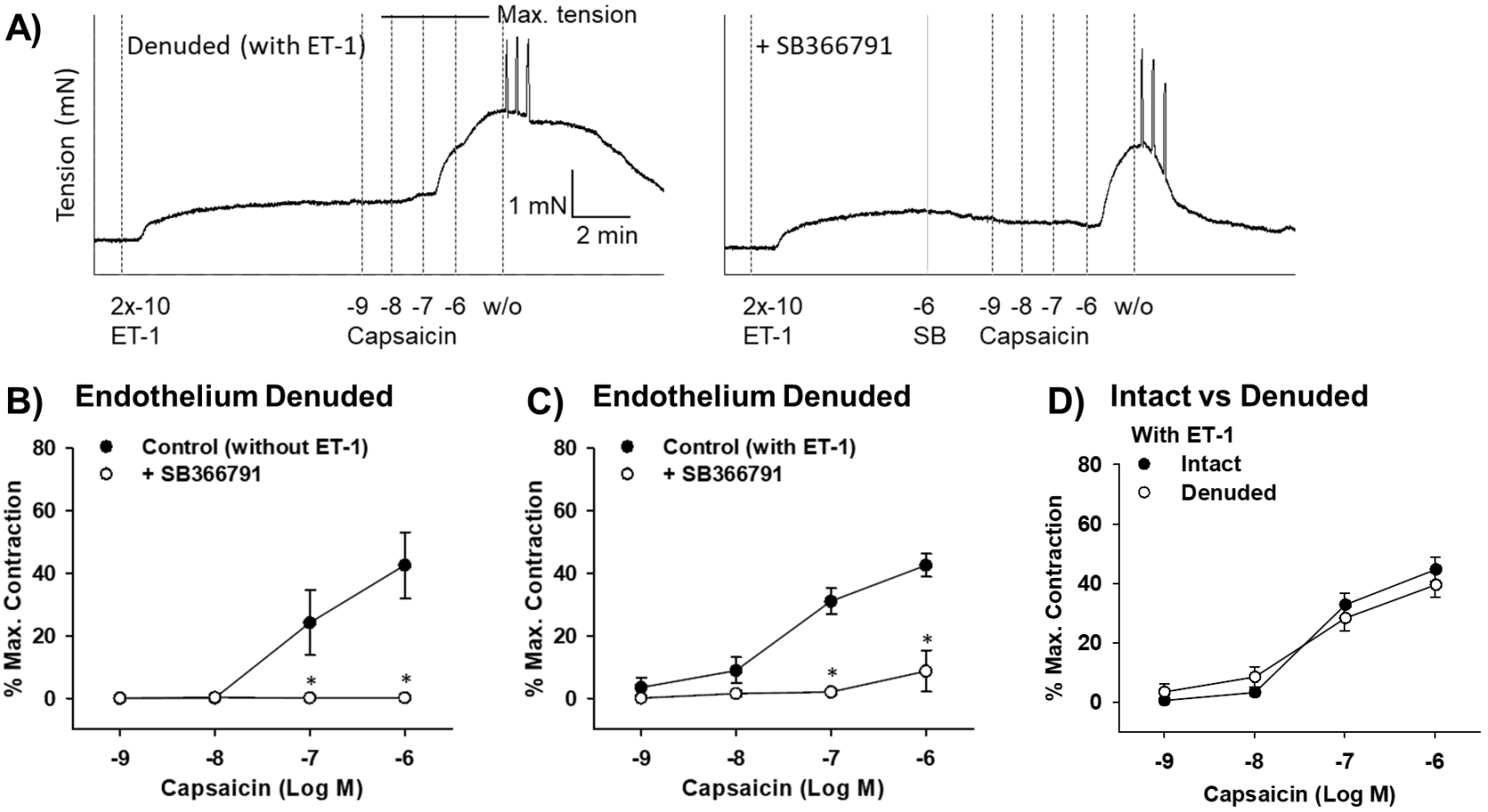
A)
Denuded (with ET-1)
Max. tension
Tension (mN)
1 mN
2 min
2x-10
ET-1
-9 -8 -7 -6 w/o
Capsaicin
+ SB366791
2x-10
ET-1
-6
SB
-9 -8 -7 -6 w/o
Capsaicin
B) Endothelium Denuded
Control (without ET-1)
+ SB366791
% Max. Contraction
Capsaicin (Log M)
C) Endothelium Denuded
Control (with ET-1)
+ SB366791
% Max. Contraction
Capsaicin (Log M)
D) Intact vs Denuded
With ET-1
Intact
Denuded
% Max. Contraction
Capsaicin (Log M)

Figure 5. Effect of ET-1 preconstriction on capsaicin-induced constriction of endothelium-denuded HAA. A) Representative wire myography traces of tension (mN) generated in ET-1 preconstricted, endothelium-denuded HAA following application of cumulative concentrations of capsaicin (1 nM-1 µM), in the absence or presence of SB366791. Concentration response curves showing percent maximum constriction of unpaired, endothelium-denuded, **B)** non-preconstricted and **C)** ET-1-preconstricted (16 ± 5 % preconstriction) HAA to cumulative concentrations of capsaicin (1 nM-1 µM). Preconstriction with ET-1 slightly potentiated capsaicin-induced constriction of endothelium-denuded HAA (31 ± 4 % at 100 nM capsaicin) as compared to non-preconstricted, endothelium-denuded HAA (24 ± 10 % at 100 nM capsaicin) but did not attain statistical significance. Preincubation of ET-1 preconstricted HAA with SB366791 significantly inhibited this potentiation response (2 ± 1 % at 100 nM capsaicin). **D)** Concentration response curves comparing percent maximum constriction of ET-1-preconstricted HAA to cumulative concentrations of capsaicin (1 nM-1 µM) between endothelium-intact and endothelium-denuded arterioles. No significant differences in capsaicin-evoked constriction were observed between endothelium-intact (45 ± 4 % at 1 µM capsaicin) and endothelium-denuded (40 ± 4 % at 1 µM capsaicin;), ET-1 preconstricted HAA. All curves were generated using wire myography. *P<0.05 by two-factor repeated measures ANOVA; n=5 vessels (Fig. 5B), n=5 vessels (Fig. 5C), n=20 intact and 6 denuded vessels (Fig. 5D), 1 vessel/patient.

Figure 6

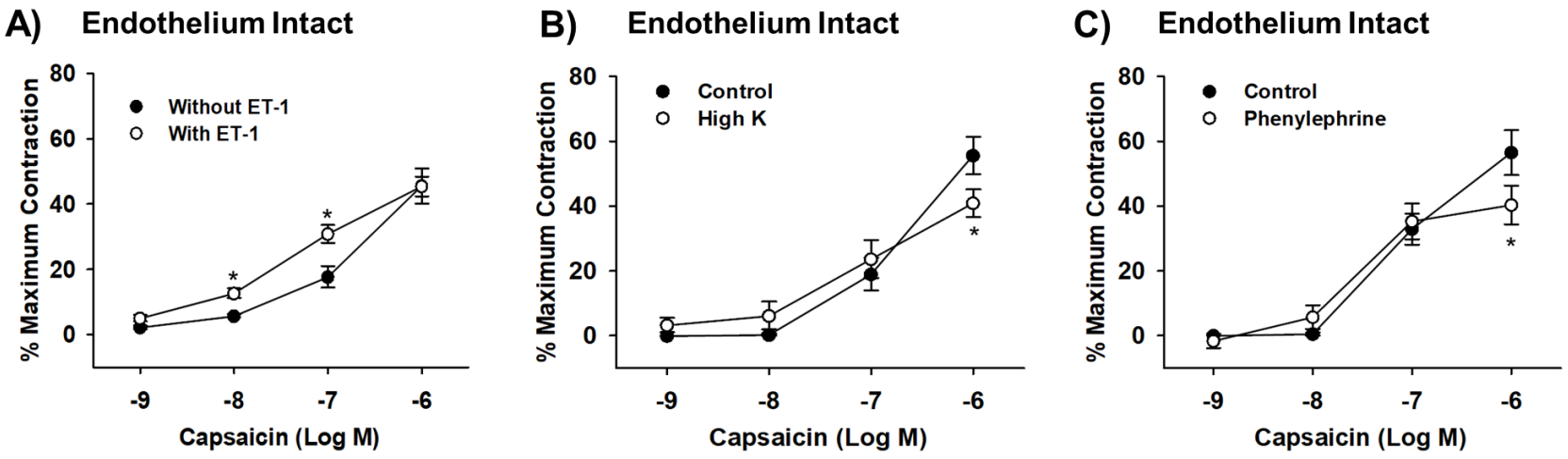

Figure 6. Effect of ET-1, high potassium PSS and phenylephrine preconstriction on capsaicin-induced constriction of endothelium-intact HAA. Concentration response curves comparing percent maximum constriction of paired, endothelium intact HAA to cumulative concentrations of capsaicin (1 nM-1 µM) between non-preconstricted (Control) and **A)** ET-1 preconstricted (24 ± 2 % preconstriction) arterioles or **B)** High-K^+ PSS-preconstricted (20 ± 3 % preconstriction) arterioles or **C)** phenylephrine-preconstricted (29 ± 3 % preconstriction) arterioles. All curves were generated using pressure myography. Preconstriction with ET-1 significantly potentiated capsaicin-induced constriction of endothelium-intact HAA (31 ± 3 % at 100 nM capsaicin) as compared to non-preconstricted HAA (18 ± 3 % at 100 nM capsaicin). Preconstriction with high-K^+ PSS did not potentiate capsaicin-induced constriction of endothelium-intact HAA (24 ± 6 % at 100 nM capsaicin) as compared to non-preconstricted HAA (19 ± 5 % at 100 nM capsaicin). Preconstriction with phenylephrine did not potentiate capsaicin-induced constriction of endothelium-intact HAA (35 ± 5 % at 100 nM

capsaicin) as compared to non-preconstricted HAA (33 ± 5 % at 100 nM capsaicin). *P<0.05 by two-factor repeated measures ANOVA; n=13 vessels from 7 patients (Fig. 6A), n=10 vessels, 1 vessel/patient (Fig. 6B), n=8 vessels, 1 vessel/patient (Fig. 6C).

Figure 7

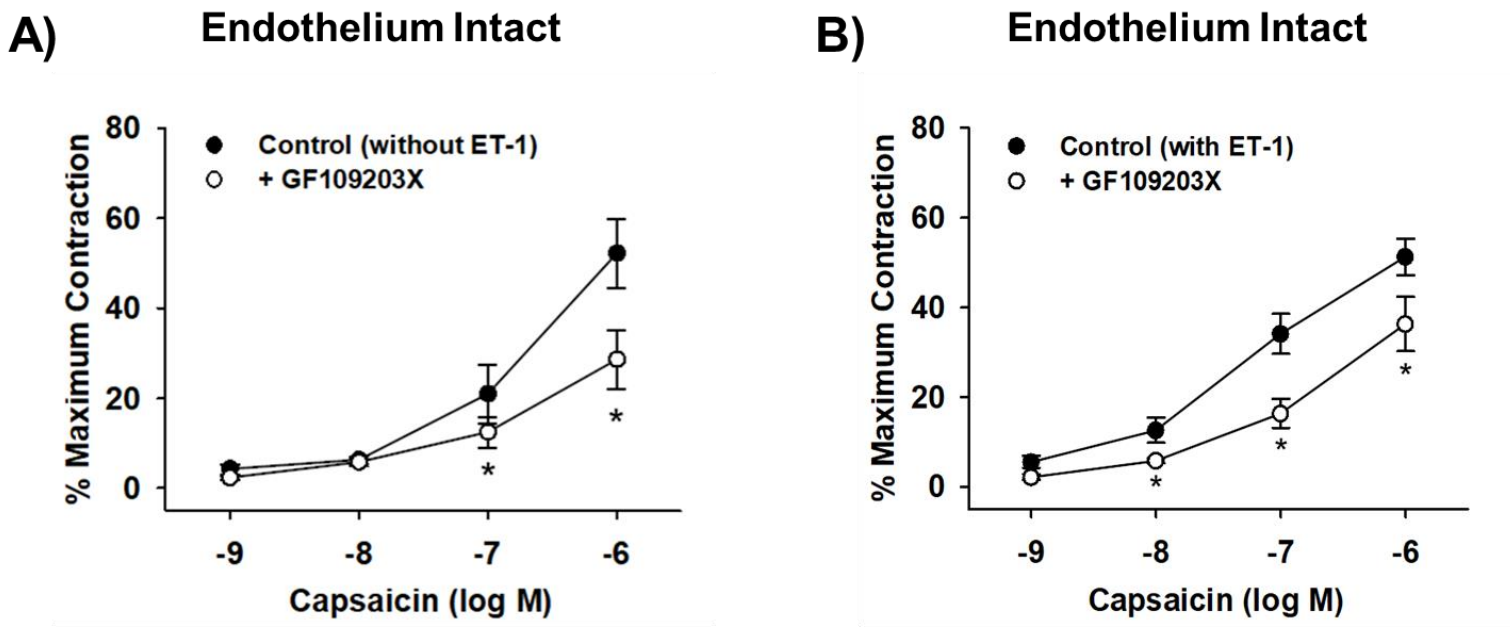

Figure 7. Effect of PKC inhibitor GF109203X on potentiation of capsaicin-induced constriction by ET-1. Concentration response curves showing percent maximum constriction of paired, endothelium-intact, **A)** non-preconstricted and **B)** ET-1 preconstricted HAA (23 ± 2 % preconstriction) to cumulative concentrations of capsaicin (1 nM-1 µM), in the absence or presence of the PKC-selective inhibitor GF109203X (1 µM). All curves were generated using pressure myography. Preincubation of ET-1 preconstricted HAA with GF109203X significantly inhibited (36 ± 6 % at 1 µM capsaicin) potentiation of capsaicin-induced constriction by ET-1 (51 ± 4 % at 1 µM capsaicin). GF109203X also significantly inhibited (29 ± 7 % at 1 µM capsaicin) capsaicin-induced constriction of non-preconstricted HAA (52 ± 8 % at 1 µM capsaicin). *P<0.05 by two-factor repeated measures ANOVA; n=5 vessels (Fig. 7A), n=6 vessels (Fig. 7B), 1 vessel/patient.

Tables

Table 1. Patient demographic information (*n*=63)

	Adipose (*n*=50)		Atrial & Donor heart (*n*=13)	
Patient demographics	non-CAD (*n*=49)	CAD (*n*=1)	non-CAD (*n*=4)	CAD (*n*=9)
Gender, Male/Female	7 (14 %)/42 (86 %)	1/0	1 (25 %)/3 (75 %)	4 (44 %)/5 (56 %)
Age, yr (mean ± SEM)	50 ± 2	59	46 ± 11	65 ± 3
Body mass index (mean ± SEM)	28 ± 1	32	34 ± 3	33 ± 3
Underlying diseases/Risk factors				
Coronary artery disease (CAD)	0	1 (100 %)	0	9 (100 %)
Hypertension	11 (24 %)	0	2 (50 %)	7 (78 %)
Hyperlipidemia	4 (9 %)	0	1 (25 %)	5 (56 %)
Diabetes mellitus	1 (2 %)	0	0	2 (22 %)
Atrial fibrillation	1 (2 %)	0	0	1 (11 %)
Congestive heart failure	0	0	0	2 (22 %)
Myocardial infarction	0	0	1 (25 %)	2 (22 %)
Cancer	9 (19 %)	0		0
None of the above	28 (57 %)	0	2 (50 %)	1 (11 %)

Table 2. Nucleotide sequence of primers

Transcript	Forward and Reverse primers	Amplicon size, bp
End-point PCR		
Human TRPV1	5'- ACG CTG ATT GAA GAC GGG AAG A -3' 5'-TGC TCT CCT GTG CGA TCT TGT T-3'	295
qPCR		
Human TRPV1	5'- TGA ACT GGA CCA CCT GGA ACA C -3' 5'- TGT CTG CCT GAA ACT CTG CTT GA -3'	118
Human PECAM-1	5'-TCA GCA GCA TCG TGG TCA ACA TA-3' 5'-GGA TGG AGC AGG ACA GGT TCA G-3'	108
Human SM22	5'-TCT GGC TGA AGA ATG GCG TGA T-3' 5'-CCA CCT GCT CCA TCT GCT TGA A-3'	123

Table 3. Characteristics of isolated, cannulated arterioles in the pressure myograph setup

	Luminal Diameter (µm)					
	Passive	Active	ET-1/ High-K^+ PSS/ Phenylephrine	Capsaicin (1 µM)	Preconstriction (%)	Number of arterioles
Adipose arterioles						
Without ET-1	162 ± 10	157 ± 10		87 ± 12		13
With ET-1	162 ± 10	158 ± 9	120 ± 9	48 ± 6	24 ± 2	13
Without High-K^+ PSS	164 ± 9	163 ± 9		76 ± 13		10
With High K+-PSS	163 ± 9	163 ± 9	130 ± 8	65 ± 10	20 ± 3	10
Without Phenylephrine	148 ± 7	144 ± 7		60 ± 7		8
With Phenylephrine	155 ± 10	152 ± 10	110 ± 10	45 ± 6	29 ± 3	8
Without GF109203X	169 ± 17	168 ± 18		81 ± 17		5
With GF109203X	169 ± 17	158 ± 17		114 ± 18		5
Without GF109203X + ET-1	156 ± 13	155 ± 13	119 ± 11	40 ± 7	23 ± 2	6
With GF109203X + ET-1	156 ± 13	151 ± 13	118 ± 11	62 ± 8	22 ± 3	6
Coronary arterioles						
With ET-1	107 ± 5	101 ± 6	67 ± 6	53 ± 6	37 ± 4	6
With ET-1 + SB366791	107 ± 6	104 ± 7	67 ± 6	70 ± 6	36 ± 2	5

Values are mean diameters ± SEM. ET-1, endothelin-1; High-K^+ PSS, high potassium buffer.